Hamiltonian systems with many degrees of freedom: Asymmetric motion and intensity of motion in phase space

Shinjo Kazumasa*
ATR Optical & Radio Communications Research Laboratories, Seika-cho, Soraku-gun, Kyoto 619-02, Japan

Sasada Tomohei†
Shonan Institute of Technology, Fujisawa 251, Japan
(Received 1 March 1996)

This paper studies the dynamics of Hamiltonian systems with many degrees of freedom by emphasizing the many-basin structure. Three-dimensional systems in general have a many-basin structure corresponding to their many stable configurations. This is in contrast to the single-basin structure of one- or two-dimensional systems including the Fermi-Pasta-Ulam model, the Lennard-Jones model, and so on. The motion of the phase point within given basins is examined depending on the type of configuration, ordered or random. The stochastic transition in which the Kol'mogorov-Arnol'd-Moser torus collapses occurs at a certain kinetic energy for ordered configurations, similar to the behavior of one- or two-dimensional systems, but not for random configurations. This suggests that the chaotic sea prevails over the phase space with random configurations. The motion of phase point among basins is described by a Bernoulli-like shift map and classified into three types of motion, depending on the magnitude of kinetic energy: types 1, 2, and 3. Furthermore, such motion is divided into two classes of motion, depending on whether or not asymmetric motion takes place. By asymmetry we mean that the motion is unidirectional to lower basins in energy. The asymmetric motion is the dynamical manifestation of ordered phases emerging from many other random ones and occurs for types 2 and 3 but not for type 1. The dynamical origin of asymmetric motion is investigated by introducing the notion of *intensity of motion in phase space*, which is measured by $\sigma=\tau_p/\tau_q$ (τ_p: the time scale of mixing dynamics in the momentum space; τ_q: the time scale of diffusion dynamics in the coordinate space). σ is expressed in terms of dynamical quantities. Our assertion that two classes of motion are separated by the decisive point $\sigma=1$ is confirmed by performing computer simulations. The asymmetric motion is attributed to the transient formation of the canonical probabilistic measure before completion of relaxation. The notion of intensity of motion in phase space is expected to help in discovering a generation principle of ordered phases of condensed matter from many random ones. The dynamical properties of type 3 are also examined and discussed in detail. [S1063-651X(96)06311-8]

PACS number(s): 05.45.+b, 05.70.Fh, 05.70.Ln, 61.20.Lc

I. INTRODUCTION

Materials conceal themselves in a wide variety of phases, not all of which have been revealed, as has been witnessed by the complexity of materials in the past decade [1,2]. Yet for any given material, a common set of interactions at the atomic or molecular level underlies all phases of the material. More than three decades ago, Anderson [3] raised a question: What is a solid? In other words, why is the ground state of almost any assemblage of atoms regular, and why are there no cases of glassy lowest energy states? More important is the fact that this question is begging for a principle of condensed phases generating from many possible configurations of atoms. Since the last decade, interest has gradually grown in the understanding of a variety of condensed phases from a deterministically dynamical point of view. In particular, Aubry [4] made an intensive study of the Frenkel-Kontorova model to find the crystalline ground state among many possible configurations of atoms depending on the parameter values involved. Besides crystalline states, there exist in nature many condensed phases including glassy states, supercooled liquids, clusters of atoms, and so on. In order to offer a unifying principle for understanding condensed phase properties of an N-atom system, Stillinger and Weber [5] advocated the approach of shifting from ordinary three-dimensional space to the $3N$-dimensional configuration space, where collective phenomena in condensed phases are determined. In his investigation of the glass-forming process, one of the authors [6] extended Stillinger and Weber's idea to find the phenomenon of the asymmetric motion of the phase point in a Lennard-Jones system. At high kinetic energy, the phase point wanders erratically over various local minima in the $3N$-dimensional configuration space. As the kinetic energy is decreased, it begins to wander erratically, but as time passes it stays for a long time at a local minimum. As time passes further, it moves to another local minimum which is lower in energy than the former.

This raises a question: Why and how is the kinetic energy frozen? In order to address this question, it is necessary to study deterministically dynamical systems. Such a study has a long history since Boltzmann invoked the ergodic hypothesis in constructing statistical mechanics. However, to our

*Present address: ATR Adaptive Communication Research Laboratories, Seika-cho, Soraku-gun, Kyoto 619-02, Japan; Electronic address: shinjo@acr.atr.co.jp

†Electronic address: sasada@la.shonan-it.ac.jp

knowledge few works have gone beyond the case where there is only one phase such as gas, liquid, or crystal; accordingly, such approaches are not sufficient to address the above question.

In this paper we repeat and extend some of the results given in the previous papers [6] and investigate the dynamical behavior of Hamiltonian systems with many degrees of freedom in which there are many local minima in the configuration space. This work has two aspects: the theory of deterministically dynamical systems and condensed matter physics. It is the former on which this paper concentrates. From the dynamical point of view, matter is the dynamical state of a Hamiltonian system that is represented by a phase point in a phase space with extremely high dimensions. From the macroscopic point of view, each visible phase is a point of the coordinate space, i.e., the configuration space embedded in the phase space. We call the region surrounding a local minimum a ''basin.'' The formation of the many-basin structure produces a variety of dynamics such as the motion among basins and that within a basin. The motion of phase point among basins is the dynamical source of the many-particle systems changing configurations and condensed matter phases. Thus, the study of motion among basins is a central issue in various fields such as the physics of dynamical systems, the physics of condensed matter (including glasses), and the physics of statistical mechanics. The number of basins depends on the spatial dimensions, the type of interaction potential, and the number of particles. The system we mainly deal with is a three-dimensional Lennard-Jones system of N particles that can cause a variety of condensed phases. However, the results given in this paper may be applied not only to the Lennard-Jones system, but to any system with a many-basin structure.

In order to describe the motion of the phase point, it is convenient to separate it into the motion within a basin and the motion among basins. The motion within a basin depends on a property of basins, namely, the particles' configuration; the motion within an amorphous structure is much more stochastic than that within a crystalline one. It has been shown that a stochastic transition takes place between ergodic and nonergodic states in the latter, while such a transition is absent in the former. The motion among basins is very complicated. It was found in a previous paper that there are three types of motion among basins depending on the magnitude of kinetic energy. Asymmetric motion takes place as the kinetic energy is decreased. By asymmetry we mean that the motion is unidirectional to lower basins in energy. Understanding this phenomenon is the main purpose of this paper.

To do this, we examine the behavior of orbits in the whole phase space in two ways. One is to examine the diffusion of a single orbit, and the other is to study the evolution of distance between nearby orbits in an initial stage. Analyzing the behavior of these quantities, we induce two time scales, τ_p and τ_q. τ_p is the time when nearby orbits forget their initial conditions, which is identical to the notion of the relaxation time for the momentum space of Krylov [7], who estimated the rate at which the orbits diverge for the hard-sphere gas. τ_q is the sojourn time of the phase point in a single basin. The ratio $\sigma=\tau_p/\tau_p$, which we call the intensity of motion in phase space, is found to control the motion among basins. When $\sigma>1$, asymmetric motion does not take place, and the motion among basins is very erratic. Conversely, when $\sigma<1$, asymmetric motion takes place, causing the volume of the momentum space to increase. The asymmetric motion is attributed to the transient formation of the canonical probabilistic measure before completion of relaxation. The notion of the intensity of motion in phase space is expected to help in discovering a generation principle of ordered phases of the condensed matter out of many random ones.

The outline of this paper is as follows. Section II presents the model and provides details on the molecular-dynamics simulation technique. A periodic boundary condition is imposed to avoid the cluster formation of particles. Section III presents results for both the motion within a basin and the motion among basins. Section IV examines the behavior of orbits in the phase space. The notion of the intensity of motion in phase space is introduced to clarify the motion among basins. Section V examines the results of computer simulations to evaluate our assertion that the decisive point of whether or not asymmetric motion takes place is given by $\sigma=1$. Section VI gives our conclusions and discusses directions for future work.

II. HAMILTONIAN SYSTEMS AND THE MANY-BASIN STRUCTURE

A. Hamiltonian

The system we consider is given by the following Hamiltonian equations;

$$H[p_{j\alpha},q_{j\alpha}]=\frac{1}{2}\sum_{j\alpha}^{Nd}\left(\frac{p_{j\alpha}^2}{m}+V[q_{j\alpha}]\right),$$

$$V[q_{j\alpha}]=\sum_{j(\neq k)}v(q_{jk}), \tag{1}$$

where m is the mass of the particle and $v(q_{jk})$ describes the interaction in which q_{jk} is the distance between particles j and k. $p_{j\alpha}$ and $q_{j\alpha}$ are the canonical conjugate variables, the α components of the momentum, and the coordinate of the jth particle. N is the number of particles, and d is the number of dimensions of the real space in which the system is embedded. $V[q_{j\alpha}]$ is the potential surface, the number of dimensions of which is equal to Nd. The phase point describing the dynamical state of the system is described by the set of $\{p_{j\alpha},q_{j\alpha}\}$, a point in the phase space or the Γ space. The number of dimensions of the Γ space is $2Nd$. Throughout this paper we use the notations j and k to number the particle and the notation i to express the time, such that $t_i=t_0+i\Delta$ in Sec. III B and $t_i=t_0+i\Delta_t$ in the Appendix, where t_0 is the initial time and Δ and Δ_t are the time steps.

Let us define the interaction potential. Two conditions are imposed on $v(q)$: (i) $-\infty<v(q)$ for any q and (ii) $v(q)<q^{-d}$ for a large q. Condition (i) ensures stable configurations of particles, while condition (ii) ensures the thermodynamics limit, excluding the inhomogeneous distribution of the particles. Condition (i) excludes Hamiltonian systems such as the celestial and the Coulombic ones from our considerations, in which the particle configuration is stabilized by the motion of the constituent particles. Throughout

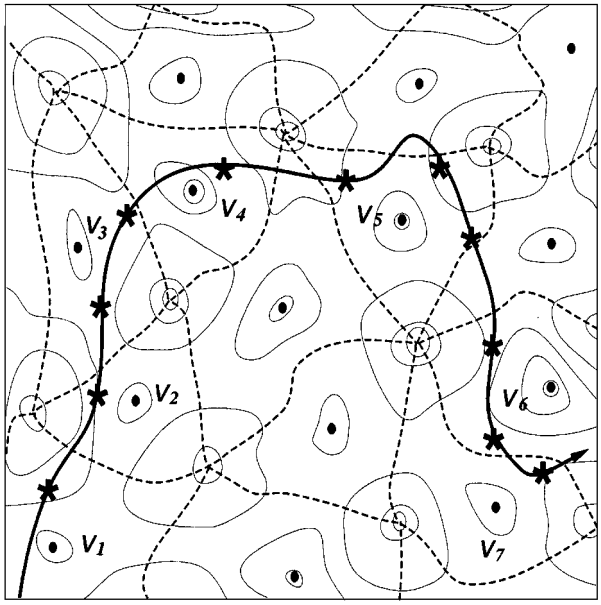

FIG. 1. The simplified topography of the potential surface $V[q_{j\alpha}]$ projected onto the two-dimensional space. The bold dots stand for the local minima, and the broken lines for the ridge lines. The region surrounded by the ridge lines is a basin. The trajectory is indicated by a bold line. As described in Sec. III B, the trajectory is generated by the Bernoulli-like shift map $V_{i+1}=\phi V_i$. V_i is the potential energy at the local minimum of the basin, satisfying the relation $V_i=V[q_{j\alpha}]/3dN$ ($V[q_{j\alpha}]$ is the total potential energy). The trajectory illustrated in this figure is presented by $\{\ldots,V_1,V_2,V_3,V_3,V_4,V_5,V_5,V_5,\ldots\}$.

a large part of this paper, the interaction potential is taken to be the Lennard-Jones (LJ) potential of the form

$$v(q)=4\epsilon_0\left[\left(\frac{l}{q}\right)^{12}-\left(\frac{l}{q}\right)^{6}\right]. \tag{2}$$

The LJ potential has a conflicting nature of interactions, so it produces a complex potential energy landscape that consists of many valleys and hills in the configuration space of the system when $N\gg 1$. The topography of the potential energy $V[q_{j\alpha}]$ is projected onto the plane as illustrated in Fig. 1. The Nd-dimensional coordinate space is divided into basins, each of which contains one minimum of $V[q_{j\alpha}]$. The bold dots stand for the local minima and the dotted lines for the ridges. The region surrounded by the ridge lines is a basin. All basins are connected, but not necessarily simply connected. The configuration of the particles within a basin is not in a stable phase in terms of thermodynamics because the potential barrier between the basins may not be extensive or the size of certain basins may be too negligible to contribute to the thermodynamical quantities.

The number $M[N]$ of the basins with different configurations increases very rapidly for larger systems [8,9]; it is at most proportional to $e^{\mu N}$, where μ is a constant depending on the system. This exponential form has the additive property of $M[N_1+N_2]=M[N_1]M[N_2]$, implying that the many-basin structure of the system consisting of (N_1+N_2) particles is produced by combining the many-basin structures of two subsystems with N_1 and with N_2. For the truncated LJ potential, the number of the basins was counted [10] and found to be $M[32]=157$, yielding $\mu\simeq 0.16$. From this value, $M[108]\simeq 3.2\times 10^7$ has been obtained for $N=108$. There is a variety of configurations, i.e., random and ordered ones. A many-particle system forms the face-centered-cubic (fcc) ordered configuration at the ground state and random configurations at higher potential energy states. The number of random configurations is overwhelmingly larger than that of the ordered configurations. When considering the motion of phase point in the Γ space, it is natural to separate its motion into that within a basin and that among basins. In what follows, we shall investigate the transient dynamical properties of the Hamiltonian system with $N\gg 1$, focusing on the many-basin structure. By transient, we mean that the observation time of the dynamical behaviors is shorter than or equal to the relaxation time. (These time scales will be discussed in Sec. III.) Then, it is helpful to ask whether or not the quantities of interest have the additive property and whether or not the quantities normalized by N vanish in the limit $N\to\infty$.

Investigations of dynamical properties are performed using the standard molecular-dynamics technique, i.e., Verlet's [11] and Runge-Kutta's algorithms. The periodic boundary condition is imposed on the system; $V[q_{j\alpha}]=V[q_{j\alpha}+n^\alpha L]$ in Eq. (1), where n^α is any integer. L is determined by using the thermodynamic relation, the virial theorem relating it with system pressure P,

$$PL^d=\frac{1}{d}\sum_{j\alpha}^{Nd} p_{j\alpha}\frac{\partial H}{\partial p_{j\alpha}}-\frac{1}{d}\sum_{j\alpha(j<k)}^{Nd} q_{j\alpha k\alpha}\frac{\partial H}{\partial q_{j\alpha k\alpha}}, \tag{3}$$

where $q_{j\alpha k\alpha}=q_{j\alpha}-q_{k\alpha}$. This is used to determine L at the initial stage by putting the system pressure P equal to zero: $P=0$. The term on the right-hand side of this equation is evaluated for the single trajectory starting from the initial condition in the Γ space, keeping the total energy constant. It is noteworthy that the ergodicity property is not assumed in Eq. (3). The virial theorem usually holds when we average the terms on the right-hand side of Eq. (3) over a long time along the single trajectory under the ergodic assumption that the time average is equal to the average of the ensemble of trajectories uniformly scattered over the whole region of the available Γ space. P does not generally keep its initial value as time elapses for the fixed L.

All the quantities for the LJ interaction are expressed in scaled form in which mass, distance, energy, and time are measured by using units of m, l, ϵ_0, and $0.01\sqrt{\{l^2\epsilon_0/m\}}$ $(=\Delta_t)$, respectively. Δ_t is the time step used in the molecular dynamics. The quantity T, defined by

$$T=\frac{2}{d}\epsilon_K \tag{4}$$

where ϵ_K is the kinetic energy per particle, is used to characterize the kinetic energy of the system, which corresponds to the temperature in the thermodynamics.

The number of particles used in the investigation of molecular dynamics is $N=4n^3$ (n is a positive integer), so the particles can have the fcc configuration. The value of N used is 32, 108, 256, 500, or 864. All calculations in this paper are performed by assuming $d=3$.

In the remaining part of this section, we study the motion of phase point within a basin.

B. Motion within a basin

In previous works, the dynamical properties have been discussed [12–17] for one- or two-dimensional systems having a single basin. The occurrence of the stochastic transition in which the Kol'mogorov-Arnol'd-Moser (KAM) torus collapses has been the main issue, which is related to the ergodic property of the system showing the equipartition law where the kinetic energy is equally distributed over the degree of freedom. The Arnol'd diffusion [18,16], the equipartition [19–21], and the Boltzmann-Jeans freezing of the high frequency mode [22–24] have been examined as dynamical characteristics of many-particle systems.

For a system having the many-basin structure, we investigate the dynamical properties of the motion within a basin. For the cases where the potential barrier separating one basin from other basins is high, the motion of phase point is confined in the initial basin. For the other cases, the phase point escapes from the basin and wanders among the basins. It is a formidable task to estimate the potential barrier height for all basins. When the kinetic energy is sufficiently small, the phase point stays in the initial basin for a long time before going to other basins. For $T \leqslant 0.05$, the phase point stays in the basin for a time of $t < 500$.

We study the dynamical instability of the trajectories of the phase point. The time evolution of the separation between the nearby trajectories is examined. A method evaluating the evolution rate of two trajectories cannot be applied because the dynamical quantities $q_{j\alpha}$ are confined within a very small region near the local minima (Fig. 1). Instead, we set up the equation of motion for small quantities $\delta p_{j\alpha}(t)[=p_{j\alpha}(t)-p^0_{j\alpha}(t)]$ and $\delta q_{j\alpha}(t)[=q_{j\alpha}(t)-q^0_{j\alpha}(t)]$ $(j=1,\ldots,N;\ \alpha=1,\ldots,d)$ along the trajectory $\{p^0_{j\alpha}(t), q^0_{j\alpha}(t)\}$. This method makes it possible to obtain the Lyapunov exponents, which are evaluated for the time before the phase point goes to other basins. Consequently, the definition of the Lyapunov exponent here is different from the usual definition, in which they are quantities averaged over long times under the ergodic assumption. (Details of the calculations are given in the Appendix.)

The growth rate is averaged over many initial conditions set in the initial basin for the system. The largest Lyapunov exponents calculated for $N=32$ and 108 are calculated: the result for $N=108$ is almost identical to those for $N=32$. In Fig. 2, the largest Lyapunov exponents for $N=108$ are shown as a function of T for the two types of the configurations of particles, ordered and random. They read

$$\lambda_r(T) \simeq 6.3(T-T_0^r), \quad T_0^r \simeq 0.0; \quad T_0^r \leqslant T \leqslant 0.05$$

for random configurations, (5)

$$\lambda_c(T) \simeq 1.2(T-T_0^c), \quad T_0^c \simeq 0.023; \quad T_0^c \leqslant T \leqslant 0.05$$

for fcc ordered configuration.

From this, we observe the following features: (1) The stochastic transition point (T_0^r or T_0^c) at which the Lyapunov exponents vanish depends on the particle configuration: it is finite for the fcc configuration, while it vanishes for the random configurations. For the fcc-ordered configuration, T_0^c is found to be insensitive to the number N of particles; thus, it is likely to remain finite even for the case $N \to \infty$. For example for the LJ systems consisting of Ar particles, T_0^c amounts to $\simeq 4.3$ K. This value agrees well with the 5 K transition energy for the two-dimensional LJ system of Ar particles with $N=64$ [25,26]. For the small kinetic energy of $T \leqslant T_0^c$, the phase point is trapped on the KAM torus. This means that the Γ space is divided into many mutually disjointed invariant measures. Most basins have random configurations. The stochastic transition point T_0^r is insensitive to the degree of randomness of configuration as well as to the system size N ($\gg 1$). It is important that the stochastic transition point T_0^r vanishes. This suggests that the volume of the Γ space occupied by the KAM torus is so small that the phase point wanders in the chaotic sea connecting most regions in the Γ space, provided that the kinetic energy is greater than the potential barrier between basins. (2) The trajectory instabilities are stronger for the random configurations than for the ordered configurations.

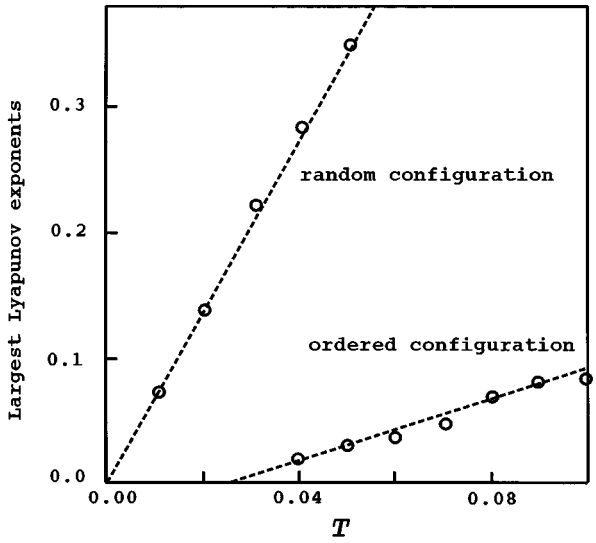

FIG. 2. The largest Lyapunov exponent as a function of T for the LJ system of $N=108$ and $d=3$ for two types of configurations; fcc ordered and random. T characterizes the kinetic energy, which is defined in Eq. (4). The unit of the horizontal axis is the energy unit ϵ_0 [appearing in Eq. (2)], and that of the vertical axis is $1/\Delta_t$, where Δ_t is the time unit: $\Delta_t = 0.01\sqrt{\{l^2\epsilon_0/m\}}$.

The spectra of Lyapunov exponents is shown in Fig. 3 for the system of $N=108$, assuming $T=0.05$. The Lyapunov exponents, whose number is $2dN$ $(=648)$, are arranged in descending order. (The method of calculations is also given in the Appendix.) The following properties are concluded for the Hamiltonian systems. The sum of them exactly vanishes, as concluded from the Liouville theorem that the phase space volume is kept constant. A pair of λ_m and $\lambda_{2dN-m+1}$ such that $\lambda_m = -\lambda_{2dN-m+1}$ $(1 \leqslant m \leqslant dN)$ always appears, as concluded from the time reversibility of the equation of motion. Among many Lyapunov exponents, $2d$ $(=6)$ pieces exactly vanish, as concluded from the translational symmetry along x, y, and z directions.

The calculated spectra show that six pieces of Lyapunov exponents do not vanish due to the bad convergence, especially for the small λ_m. It is found that the gap near $\lambda_m = 0$ becomes narrower as the run time is extended; the existence of the gap is attributed to the method in which the transla-

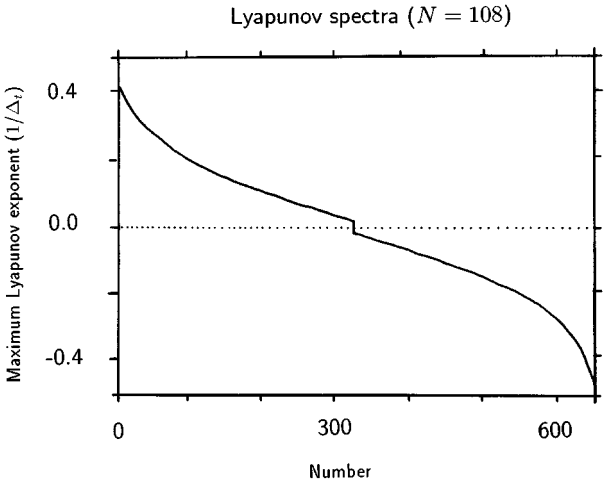

FIG. 3. The Lyapunov spectra for the LJ system with $N=108$ and $d=3$ with $T=0.05$. The Lyapunov exponents numbered by a positive integer less than or equal to $2dN$ $(=648)$ are arranged in larger order. The unit of the vertical axis is $1/\Delta_t$, where Δ_t is the time unit: $\Delta_t=0.01\sqrt{\{l^2\epsilon_0/m\}}$.

tional symmetry of the Hamiltonian is not taken into account. The shape of the spectra does not change drastically as the run time is extended. The magnitude of the largest Lyapunov exponents agrees well with that shown in Fig. 2. These observations imply that the overall shape of the spectra and the magnitude of the largest Lyapunov exponents are reliably consistent. The spectra are downwardly convex for the positive region $\lambda_m>0$. This implies that in the Γ space the directions along the trajectory are divided into two distinct directions, those with strong instability and those with weak instability. The shape of the Lyapunov spectra is also insensitive to the degree of randomness of configuration.

III. LANDSCAPE DYNAMICS

A. Two time scales and observation time

We study the inherent dynamics of the many-basin structure, the motion of phase point among basins. First of all, we note that there are two types of time scales for the many-particle systems, i.e., recurrence time and relaxation time. One is the Poincaré recurrence time [27]. For the system with a fixed Nd and finite volume of Γ space, the phase point returns to near the initial point after a certain time. The expression for the recurrence time $\tau_{\rm recur}$ averaged over the repeated recurrence of the single trajectory was formulated by Smolukhovsky [28]. For systems of mixing type, the recurrence time becomes proportional to the volume of the phase space, $\tau_{\rm recur}\simeq e^{\theta N}$, where θ depends on the resolution of the measurement for our observation. For the macroscopic system with large N, the recurrence time becomes very large. Boltzmann [29] used this to explain why there is no occurrence of reversibility of the dynamics under our observation time. The other time scale is the relaxation time after which the ensemble of trajectories tends to be approximately uniformly distributed over the available Γ space. It was explicitly estimated by Krylov [7] for the simple model of the perfect gas to be $\tau_{\rm relax}\simeq mL^2/4h$, where h is the Planck constant and L the linear size of the system. This model has a flat potential surface; each particle changes its direction of velocity with time but keeps its magnitude constant. The relaxation time is related to the ensemble of trajectories, whereas the recurrence time is concerned with a single trajectory. For systems with many-basin structures, the magnitude of velocity as well as its direction changes for each particle. It is a formidable task to estimate the relaxation time for such systems because of the lack of a general method to confirm the completion of the relaxation process. The relaxation time may be extremely long, as is seen for the glassy phases. In the following subsection, we shall observe the motion of phase point among basins for the observation time, satisfying the relation $0<\tau_{\rm ob}\leqslant\tau_{\rm relax}$ $(\ll\tau_{\rm recur})$.

B. Shift-map description

The trajectory is described by a set of $\{p_{j\alpha}(t),q_{j\alpha}(t)\}$ for a continuous time t. Change in the configuration is produced by the motion among basins in the potential energy surface. For this, it is convenient to characterize the motion by using the basin to which the phase point belongs. The method of mapping the trajectory onto the basin was invented by Stillinger and Weber [10,5]. The configuration at the local minimum of the basin is called the inherent structure. Their method is used here to obtain the Bernoulli-like shift-map description for the motion among basins, thus allowing classification of the motion among basins. Let us consider the series of phase points measured at every predetermined time: $\{p_{j\alpha}(t_0+i\Delta),q_{j\alpha}(t_0+i\Delta)\}$ $(i=1,2,...)$. (Note that the notation i is used to express the time, but not the particle number). The series given by a set of $\{q_{j\alpha}(t_0+i\Delta)\}$ is numbered depending on which basin the phase point belongs to; the basin for the phase point starting at time $t=t_0$ is represented by the number 1. The basin at next time $t_0+\Delta$ is represented by 2 (or 1) if it is different from (or the same as) basin 1. The basin at time $t_0+2\Delta$ is represented by 3 if it is different from the previous basins 1 and 2, and represented by 1 (or 2) if it is the same as basin 1 (or 2). By repeating this procedure, the trajectory is described by a series of numbers (the value of Δ is appropriately chosen so as to characterize the motion, which is fixed during simulations):

$$n_{i+1}=\Phi n_i\,. \tag{6}$$

The shift-map description is based on the facts that the potential surface has many basins whose numbers are larger than 1 and that it is divided into the basins without overlap.

By expressing Eq. (6) in terms of the series of potential energy (denoted by V_i) at the local minimum of the basin instead of n_i, we have another Bernoulli-like shift map,

$$V_{i+1}=\phi V_i\,. \tag{7}$$

This description clarifies the correspondence between the trajectory and the potential surface. The shift-map description is illustrated in Fig. 1. The trajectory is generated by the shift map $V_{i+1}=\phi V_i$. In this figure, the trajectory is indicated by a bold line. The trajectory is expressed by a series of $\{...,V_1,V_2,V_3,V_3,V_4,V_5,V_5,V_5,...\}$. The symbols $(*)$ on the trajectory correspond to $t_i=t_0+i\Delta$. The second method will be used hereafter.

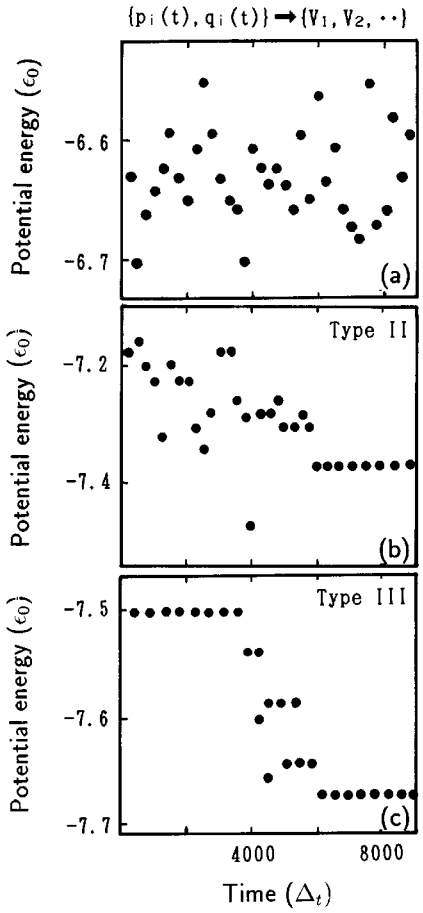

FIG. 4. Three types of motion among basins, depending upon the quantity T in descending order. All types of motion are chaotic. The trajectory $\{p_{j\alpha}(t),q_{j\alpha}(t)\}$ is described by series of V_i, as described in Eq. (7). V_i is the potential energy at the local minimum of the basin, defined by the relation $V_i=V[q_{j\alpha}]/3dN$ ($V[q_{j\alpha}]$ is the total potential energy). The unit of the horizontal axis is the time unit Δ_t ($=0.01\sqrt{\{l^2\epsilon_0/m\}}$), and that of the vertical axis is the energy unit ϵ_0 [in Eq. (2)].

C. Three types of motion among basins

Let us examine the motion of the phase point which is initially in a certain random configuration. The motion of phase point starting from ordered configurations is a process of going from the initial ordered configuration to the final state observed for random configurations. The final states are the same, regardless of the type of initial configuration, whether ordered or random. The motion among basins is classified [30,6] into three types, depending upon the quantity T in descending order of kinetic energy [Figs. 4(a)–4(c)]. All types of motion are chaotic, as seen from the fact that the largest Lyapunov exponents are positive.

1. Type 1 (wandering)

For higher kinetic energy, the phase point wanders from basin to basin and has no tendency to cease wandering. The number $s(t)$ of the basins on which the phase point passes during time interval t is scaled [10] by

$$s(t)=Nc(T)t. \tag{8}$$

The $c(T)$ measures the number of basins over which a single particle crosses during the unit time Δ_t. Note that $c(T)$ is intensive while $s(t)$ is extensive. For the system of $N=108$, $c(T)$ is numerically calculated as

$$c(T)\simeq\frac{\sqrt{T}}{5.82}\,e^{-2.16/T}. \tag{9}$$

The wandering property is clearly seen by examining the property averaged over a long time interval, as shown in Figs. 5(a)–5(c). In these, V_{i+1} is plotted as a function of the preceding V_i's. The V_{i+1}'s are distributed randomly around the line $V_{i+1}=V_i$, implying that the phase point wanders without converging toward a definite value. The points appearing on the diagonals mean that the phase point stays in the same basin at times t_i and t_{i+1}.

2. Type 2 (asymmetric motion and wandering)

For intermediate kinetic energy, the behavior of the phase point for the time interval $t<\tau_2$ is similar to that of type 1. The $s(t)$ and $c(T)$ are precisely the same as those given in Eqs. (8) and (9). The dynamics proceed toward lower V_i; the kinetic energy T increases with time. This motion, hereafter, is called *asymmetric* motion. The asymmetric motion occurs for both types 2 and 3, and is also a process of generating heat. The configuration of the particles becomes ordered as the asymmetric motion proceeds. The wandering ceases after a long time elapses for the finite N, as seen in Fig. 5(b). This ceasing time τ_2 depends on both the system size N and T: $\tau_2(N,T)$. The simulations show that $\tau_2(N,T)$ increases gradually with N and becomes rapidly shorter as T decreases. The magnitude of the largest Lyapunov exponent, measured for the finite time interval, becomes smaller as the asymmetric motion proceeds; this magnitude in the final state is roughly two-thirds of that in the initial state.

The asymmetric motion is irreversible [31] since it is chaotic. However, the irreversible motion is not always asymmetric since irreversible behavior occurs even for the motion of type 1.

3. Type 3 (intermittency and asymmetric motion)

For lower kinetic energy, the wandering property is strongly suppressed. The phase point assumes the different V_i's intermittently [Fig. 4(c)]. As T decreases, the time interval τ_3 for which the phase point stays in a single V_i becomes rapidly longer; its T dependence remains unknown because of the strong dependence of the trajectory (initial condition). This type of motion is also asymmetric motion. The dynamical behavior of this type depends strongly on the initial conditions, which were discussed in the last section. The magnitude of the largest Lyapunov exponent, which is measured for the finite time interval, behaves similar to that for type 2.

In the next section we discuss the dynamical origin of the asymmetric motion of the phase point.

IV. ASYMMETRIC MOTION

A. Two time scales

Why does asymmetric motion occur for types 2 and 3 but not for type 1? As mentioned previously, our observation

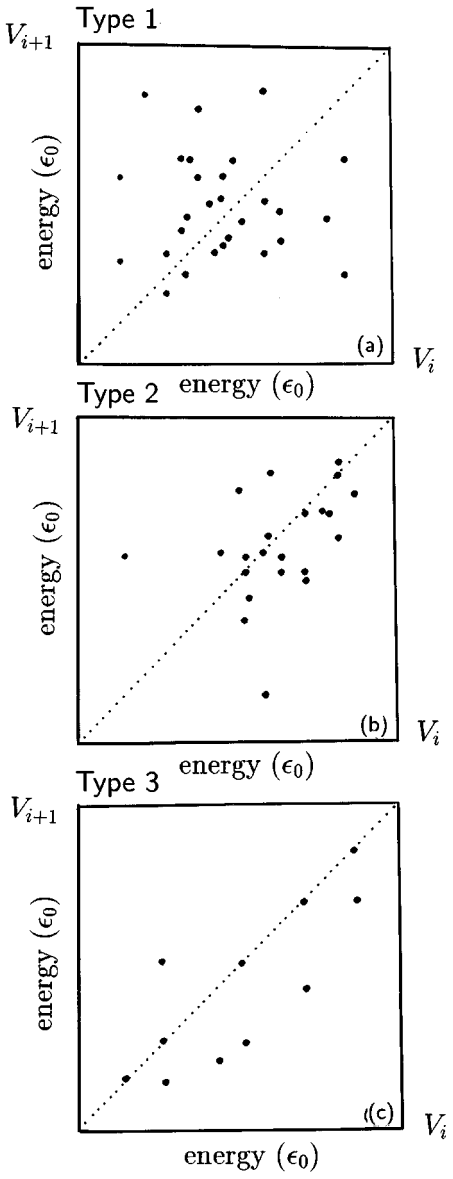

FIG. 5. (a) A plot of V_{i+1} as a function of the preceding V_i, which is obtained from Fig. 4(a) V_i is the potential energy at the local minimum of the basin, satisfying the relation $V_i = V[q_{j\alpha}]/3dN$ ($V[q_{j\alpha}]$ is the total potential energy). The unit of the horizontal axis is the same as that of the vertical axis but arbitrary. V_{i+1}'s are distributed randomly around the line $V_{i+1} = V_i$, showing that the phase point wanders without converging toward the definite values. (b) A plot of V_{i+1} as a function of the preceding V_i, similar to (a), which is obtained from Fig. 4(b). The number of dots below the line $V_{i+1} = V_i$ is larger than that above the line, showing the occurrence of the asymmetric motion. There are also some dots above the line $V_{i+1} = V_i$, showing the wandering property. (c) A plot of V_{i+1} as a function of the preceding V_i, similar to (a), which is obtained from Fig. 4(c). The number of dots below the line $V_{i+1} = V_i$ is overwhelmingly larger than that above the line, showing that the transition is dominant for the case $V_{i+1} < V_i$.

time is much less than the recurrence time: $\tau_{\rm ob} \ll \tau_{\rm recur}$. For the opposite case $\tau_{\rm recur} \ll \tau_{\rm ob}$, no asymmetric motion occurs for any Hamiltonian systems due to the the Poincaré recurrence phenomenon.

In order to address this question, let us consider two extreme cases: one is the case where the phase point stays in one basin for a long time before the subsequent transition to other basins; the other is the opposite case where it passes over each basin within a very short time interval.

For the former case, the particles frequently change their momenta in the basin so that each particle takes various values of momentum. Consequently, the sojourn time (or probability) in which the phase point stays in the domain $\Pi_{j\alpha} dq_{j\alpha}$ of the basin is given [31] by the number of microstates, i.e., the volume fraction Ω in the Γ space. Ω is calculated as

$$\Omega = \frac{\Pi_{j\alpha} dq_{j\alpha}}{h^{Nd} N!} \int \Pi dp_{j\alpha} \delta(\epsilon - H[p_{j\alpha}, q_{j\alpha}]),$$

$$= \Omega_p(\epsilon - V[q_{j\alpha}]) \Pi_{j\alpha} dq_{j\alpha}, \tag{10}$$

where

$$\Omega_p(\epsilon - V[q_{j\alpha}]) = C(N,d)(\epsilon - V[q_{j\alpha}])^{Nd/2-1}. \tag{11}$$

ϵ is the total energy of the system, and $\delta(...)$ in Eq. (10) is the Dirac function. The mixing property is assumed to obtain Eq. (10); the particles frequently exchange their kinetic energies. The prefactor $C(N,d)$ on the right-hand side of Eq. (11) depends upon d and N but not upon ϵ and $q_{j\alpha}$. Integrating Eq. (10) with respect to the coordinate $q_{j\alpha}$ under the condition $0 \leqslant \epsilon - V[q_{j\alpha}]$ obtains the total volume of the available Γ space, from which we get the Boltzmann entropy defined in statistical physics. In comparing the phase space volume at the potential energy $V[q_{j\alpha}]$ with that at $V[q_{j\alpha}] + \Delta V$, ΔV is assumed to be smaller than $\epsilon - V[q_{j\alpha}]$ at about $\Delta V \simeq 0(1)$. The volume ratio γ is given from Eq. (11) by

$$\gamma = \frac{\Omega_p(\epsilon - V[q_{j\alpha}] - \Delta V)}{\Omega_p(\epsilon - V[q_{j\alpha}])},$$

$$\simeq \left(1 - \frac{\Delta}{\epsilon - V[q_{j\alpha}]}\right)^{(Nd/2)-1}. \tag{12}$$

By using the relation $\epsilon - V[q_{j\alpha}] = NdT/2$ [see Eq. (4) for the definition of T] and assuming $1 \ll Nd$, we have the well known canonical measure for the coordinate space,

$$\gamma = \exp\left(-\frac{\Delta V}{T}\right). \tag{13}$$

The phase space volume in the Γ space becomes larger as the potential energy $V[q_{j\alpha}]$ decreases. In other words, the probability of the phase point moving in the direction of lower potential energy is larger than that in the opposite direction. Thus, we might expect the occurrence of asymmetric motion in this case (Fig. 6). The crucial point of this argument is that the canonical probabilistic measure is formed transiently unless the phase point moves over the whole region of the Γ space. Achievement to the true equilibrium state is not necessary. Ergodic assumption is expected to hold for the $\tau_{\rm relax} \leqslant \tau_{\rm ob}$.

On the other hand, for the latter case the phase point passes through a given basin without significantly changing the momenta of the particles. Therefore, the sojourn time where the phase point stays in the domain $\Pi_{j\alpha} dq_{j\alpha}$ of the basin is no longer given by Eq. (10). There are two cases where the sojourn time is given by Eq. (10): the first is the case we deal with, as discussed above; the other is the case where relaxation to the equilibrium state is accomplished. In

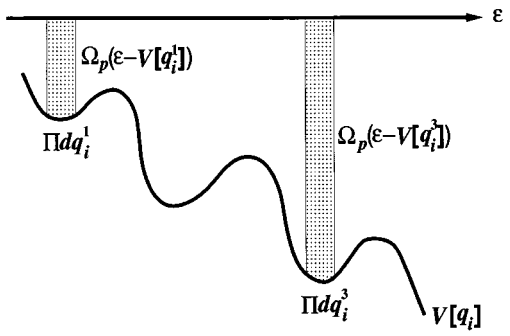

FIG. 6. Occurrence of the asymmetric motion. The horizontal axis describes the configuration space, while the vertical axis shows the potential energy. The following inequality holds: $\Omega_p(\epsilon - V[q_{j\alpha}^3]) < \Omega_p(\epsilon - V[q_{j\alpha}^1])$ when $V[q_{j\alpha}^1] > V[q_{j\alpha}^3]$. Here, $\Omega_p(\epsilon - V[q_{j\alpha}])$ is the volume of Γ space when the volume of the coordinate space is equal to unity. ϵ is the total energy of the Hamiltonian. The probability of the phase point occupying a unit volume of the coordinate space may be proportional to $\Omega_p(\epsilon - V[q_{j\alpha}])$. The probability of the phase point moving in the direction of lowering the potential energy is larger than that in the opposite direction. Thus, we expect that the motion is unidirectional to lower basins in energy, i.e., the occurrence of the asymmetric motion.

the latter case, relaxation time must be much shorter than the observation time. However, this contradicts our assumption made in Sec. III A.

The arguments above suggest that there are two distinct time scales, depending on whether or not the probabilistic measure is formed transiently. One is the time scale τ_p, during which mixing is accomplished in the momentum space. The other is τ_q, during which the phase point passes though a given basin. Before evaluating the two time scales, we examine the behavior of the dynamical variables $p_{j\alpha}$ and $q_{j\alpha}$ in the next subsection.

B. Absolute and relative diffusions: Existence of the crossover time τ_c

The absolute and relative diffusions, $a_{p,q}(t)$ and $r_{p,q}(t)$, are, respectively, defined by

$$\begin{aligned} a_{p,q}(t)^2 &= a_p(t)^2 + a_q(t)^2, \\ r_{p,q;p',q'}(t)^2 &= r_{p,p'}(t)^2 + r_{q,q'}(t)^2, \end{aligned} \tag{14}$$

where

$$\begin{aligned} a_p(t)^2 &= \frac{1}{Nd}\left\langle \sum_{j\alpha} \left| p_{j\alpha}(t) - p_{j\alpha}(0) \right|^2 \right\rangle, \\ a_q(t)^2 &= \frac{1}{Nd}\left\langle \sum_{j\alpha} \left| q_{j\alpha}(t) - q_{j\alpha}(0) \right|^2 \right\rangle, \end{aligned} \tag{15}$$

$$\begin{aligned} r_{p,p'}(t)^2 &= \frac{1}{Nd}\left\langle \sum_{j\alpha} \left| p_{j\alpha}(t) - p'_{j\alpha}(t) \right|^2 \right\rangle, \\ r_{q,q'}(t)^2 &= \frac{1}{Nd}\left\langle \sum_{j\alpha} \left| q_{j\alpha}(t) - q'_{j\alpha}(t) \right|^2 \right\rangle. \end{aligned} \tag{16}$$

Two trajectories described by the set $\{p_{j\alpha}(t), q_{j\alpha}(t)\}$ and the set $\{p'_{j\alpha}(t), q'_{j\alpha}(t)\}$ are close to each other at the initial time $t=0$. The $\langle \cdots \rangle$ stands for the average over the ensemble of the trajectories starting from the small region ω in the Γ space. Consequently, these quantities also depend on the initial conditions. The suffixes p, q, p', and q' of the diffusion lengths defined by Eqs. (15) and (16) are ambiguous because they are averaged over the ensemble of trajectories $\{p_{j\alpha}(t), q_{j\alpha}(t)\}$, and so have no dependence on each trajectory. However, the addition of these suffixes help to get the following triangle inequalities. First we consider a diffusion length analogous to those in Eqs. (15) and (16) for two trajectories [the quantities without brackets in Eqs. (15) and (16)], which results in the triangle inequalities analogous to those in Eqs. (17) and (18) for those trajectories. Next, we average the resultant inequalities over the ensemble of the trajectories starting from region ω to get the following inequalities:

$$r_{q,q'}(t)^2 \leqslant a_q(t)^2 + a_{q'}(t)^2 + r_{q,q'}(0)^2, \tag{17}$$

$$r_{p,p'}(t)^2 \leqslant a_p(t)^2 + a_{p'}(t)^2 + r_{p,p'}(0)^2. \tag{18}$$

Together with these, we also have

$$r_{p,q;p',q'}(t)^2 \leqslant a_{p,q}(t)^2 + a_{p',q'}(t)^2 + r_{p,q;p',q'}(0)^2. \tag{19}$$

The numerical calculations performed for the systems of $N=32$, 108, 256, and 864 show that the absolute and relative diffusions have the following properties:

$(p1)$ For large t,

$$a_q(t)^2 = \tfrac{1}{2} D_q(T) t, \tag{20}$$

where $D_q(T)$ is the diffusion length.

$(p2)$ All of the relative diffusion lengths increase exponentially with time for short t [32] as

$$\begin{aligned} r_{p,q;p',q'}(t)^2 &\simeq r_{p,q;p',q'}(0)^2 e^{2\lambda_r t}, \\ r_{p,p'}(t)^2 \simeq r_{p,p'}(0)^2 e^{2\lambda_r t}, &\quad r_{q,q'}(t)^2 \simeq r_{q,q'}(0)^2 e^{2\lambda_r t}, \end{aligned} \tag{21}$$

where λ_r is the largest Lyapunov exponent.

$(p3)$ $r_{p,p'}(t)^2$ saturates at a certain time.

$(p1)$ is the property seen for normal liquids. $(p2)$ is what is expected because all motions are chaotic, as seen in Sec. III C. $(p3)$ is concluded from the following inequality:

$$r_{p,p'}(t)^2 \leqslant \left\langle \frac{1}{Nd} \sum_{j\alpha} \{ p_{j\alpha}(t)^2 + p'_{j\alpha}(t)^2 \} \right\rangle + r_{p,p'}(0)^2, \tag{22}$$

$$\leqslant \left\langle \frac{2}{d} (\epsilon_K + \epsilon'_K) \right\rangle + r_{p,p'}(0)^2 \simeq 2T + r_{p,p'}(0)^2. \tag{23}$$

The upper boundedness of $r_{p,p'}(t)^2$ comes from the fact that the Hamiltonian has the monotonically increasing (quadratic) function of the variables $p_{j\alpha}$ and from the fact that the kinetic energy is positive while the potential energy is lower bounded: $-\infty < V[q_{j\alpha}]/N$. It follows from $(p2)$ and $(p3)$

that there exists a crossover time τ_c of $r_{p,p'}(t)^2$ between short and long times such that

$$r_{p,p'}(t)^2 \simeq r_{p,p'}(0)^2 e^{2\lambda_r t} \quad \text{for } 0 \leqslant t < \tau_c, \tag{24}$$

$$r_{p,p'}(t)^2 \simeq 2T + r_{p,p'}(0)^2 \quad \text{for } \tau_c < t. \tag{25}$$

From these, we easily obtain the time τ_c at which $r_{p,p'}(t)^2$ reaches its upper-bounded value:

$$\tau_c \simeq \frac{1}{2\lambda_r(T)} \left[\ln\left(\frac{2T}{r_{p,p'}(0)^2} \right) \right]. \tag{26}$$

[See Eq. (16) for the definition of $r_{p,p'}(0)^2$]. Here, we explicitly express the T dependence of the largest Lyapunov exponent, $\lambda_r = \lambda_r(T)$. This expression means that the τ_p is the time scale in which the initial indeterminacy of the variables $p_{j\alpha}$ increases to coincide with the basin size on the momentum space. In obtaining the equality in Eq. (26), we ignored the small term $r_{p,p'}(0)^2$ on the right-hand side of Eq. (25), instead using for comparison the remaining term $2T$ [see Sec. V for the evaluation of $r_{p,p'}(0)^2$].

A question arises: What does the existence of τ_c mean? In order to address this question, we consider two trajectories whose momenta are, respectively, given by the sets $\{p_{j\alpha}(t)\}$ and $\{p'_{j\alpha}(t)\}$. Suppose $\{p_{j\alpha}(t)\}$ are very close to $\{p'_{j\alpha}(t)\}$ at time $t=0$. For short t, the difference between the two sets is small, and so the two sets closely match. As time goes on, however, the difference between them increases, and results in vanishing the correlation at τ_c. Then, two sets behave independently. In other words, trajectories become Markovian in the momentum space [33]. Thus, τ_c is the signature of trajectories becoming Markovian in the momentum space beyond τ_c. The τ_c is also the crossover time such that

$$r_{q,q'}(t)^2 \simeq r_{q,q'}(0)^2 e^{2\lambda_r t} \quad \text{for } 0 \leqslant t < \tau_c, \tag{27}$$

$$r_{q,q'}(t)^2 \simeq r_{q,q'}(0)^2 e^{2\lambda_r \tau_c} + D_q(T)(t - \tau_c) \quad \text{for } \tau_c < t. \tag{28}$$

The monotonic increase of $r_{q,q'}(t)^2$ for large t ($\gg \tau_c$) is significant since $r_{p,p'}(t)^2$ saturates at a certain time. It is interesting to note from numerical calculations that when the Markovian process occurs in the momentum space, the diffusion lengths in the coordinate space sets obey the normal diffusion law.

It is noteworthy that the expression for the crossover time τ_c given here is equivalent to the relaxation time with respect to momenta in the Γ space estimated by Krylov [7]. He estimated the relaxation time of the system explicitly for the case of a perfect gas, based on the instability of the trajectories. By applying the arguments analogous to those made here concerning the total momentum, he obtained the relaxation time with respect to momenta except for the negligible factor,

$$\tau_{\text{Krylov}} = \frac{3/2}{\ln(\lambda_r / r_0)} \left[\ln\left(\frac{2\pi}{\Delta p_0 / p_0} \right) \right], \tag{29}$$

where $\ln(\lambda_r / r_0)$ describes the deviation rate of the total momentum from the initial value, p_0 is the momentum, and Δp_0 the initial indeterminacy. In the notations used here, $\ln(\lambda_r / r_0)$ is the largest Lyapunov exponent, p_0 is $\sqrt{T/2}$, and Δp_0 is $r_{p,p'}(0)$.

C. Intensity of motion

We are now in a position to explore the dynamical origin of the asymmetric motion. To this end, we introduce a new notion, the intensity of motion [34] in phase space, to describe the dynamical competition between the motion of the phase point in the momentum space and that in the coordinate space. The degree of intensity of motion is measured by

$$\sigma(T) = \frac{\tau_p(T)}{\tau_q(T)}, \tag{30}$$

where the $\tau_p(T)$ and $\tau_q(T)$, which were introduced in Sec. IV A, denote, respectively, the time scale characterizing the mixing of the phase point in the momentum space, and the time scale of the diffusion of the phase point in the coordinate space. Here we explicitly represented the T dependence of the quantities appearing for the expression. The $\sigma(T)$ must be intensive. The intensity of motion has the following meaning. For $\sigma(T)<1$, relaxation occurs faster in the momentum space than in the coordinate space. The phase point takes the various states inside the momentum space, forming transiently the canonical measure given in Eq. (13). In other words, the kinetic energy plays a role as *heat*. On the other hand, for $\sigma(T)>1$, the phase point transmits between the basins of the potential surface before relaxation with respect to the momentum space.

Our assertion is as follows: asymmetric motion takes place in the case $\sigma(T)<1$, and wandering motion takes place in the case $\sigma(T)>1$. The transition point determining whether or not asymmetric motion takes place is given by the boundary $\sigma(T^*)=1$.

Let us express the $\sigma(T)$ in terms of the dynamical quantities obtained in previous sections. We begin with τ_p. It is evident from arguments given in Sec. IV B that τ_p can be regarded as τ_c. Next we consider τ_q. The mean size of a basin is denoted by l_q or L_q: the capital letter L_q describes the size of the basins in the Γ space, and the lower case letter l_q describes the size of the basins normalized for one degree of freedom of the systems; L_q and l_q satisfy the relation $L_q^2 = N d l_q^2$. τ_q is the time scale where the ensemble of the phase points pass over the basin. From this, we have $L_q^2 = N d D_q(T) \tau_q$, or

$$\tau_q = \left(\frac{L_q^2}{Nd} \right) \frac{1}{Dq(T)}, = \frac{l_q^2}{D_q(T)}. \tag{31}$$

From this expression, it is seen that τ_q is the time scale where one particle jumps between two neighboring basins, the distance of which is given by l_q. By inserting Eqs. (31) and (26) into (30), we have

$$\sigma(T)=\frac{\tau_p}{\tau_q},$$

$$=\left(\frac{1}{l_q^2}\right)\frac{D_q(T)}{2\lambda_r(T)}\left[\ln\left(\frac{2T}{r_{p,p'}^2(0)}\right)\right]. \tag{32}$$

The $\sigma(T)$ given here becomes intensive, as required. It is, however, difficult to evaluate the size of the basin l_q in this expression within the limits of our computer power. Let us rewrite this expression, based on the phenomenological arguments as follows.

As seen above, τ_q describes the time interval in which the particle jumps between two neighboring basins, the distance of which is given by l_q. Recall that the number of basins over which the phase point passes during the time interval t is given by Eq. (8). The system consists of the N particles. During the time interval τ_q, some particles stay in the basin and the others jump to the next basin. Therefore, we may obtain the equation $s(\tau_q)\simeq N$ in (8), indicating that during the time interval τ_q the N particles may jump between two neighboring basins. This seems to be supported by the fact that the diffusion constant $D_q(T)$ is given by the Arrhenius law, as will be given later [Eqs. (36) and (39)]. We have $s(\tau_q)=Nc(T)\tau_q\simeq N$, from which

$$\tau_q\simeq\frac{1}{c(T)}. \tag{33}$$

By combining Eqs. (33) and (26), we have

$$\sigma(T)\simeq\frac{c(T)}{2\lambda_r(T)}\left[\ln\left(\frac{2T}{r_{p,p'}(0)^2}\right)\right]. \tag{34}$$

The $\sigma(T)$ obtained here is also the intensive. Furthermore, as will be seen later, the calculated T dependences of $D_q(T)$ and $c(T)$ are identical within the error of the simulations, indicating that the $\sigma(T)$ in Eq. (34) is the same T dependence as that in Eq. (26). This suggests the validity of our phenomenological arguments made above. The quantities $D_q(T)$ and $c(T)$ in Eq. (34) can be calculated with the results of computer simulations. Thus, we can compare the transition point of $\sigma(T^*)=1$ with the simulation results.

In the next section we evaluate our assertion by carrying out numerical calculations. Before proceeding, it should be noted that the size of a basin in the coordinate space, L_q, can be known. By comparing Eq. (34) with Eq. (32), we have the size of the basin,

$$l_q^2\simeq\frac{D_q(T)}{c(T)}\quad\text{or}\quad L_q^2\simeq Nd\left[\frac{Dq(T)}{c(T)}\right]. \tag{35}$$

This expression for the basin size is based on the phenomenological arguments.

V. RESULTS OF COMPUTER SIMULATIONS

A. Lennard-Jones systems: Case of $N=108$

The quantities $c(T)$ and $\lambda_r(T)$ in the expression in Eq. (34) are not averaged over a long time, as seen from our arguments. The dynamical behavior near the transition point determines the transition point T^* of $\sigma(T^*)=1$, so that the asymmetric motion appears long after the phase point wanders among the various basins just below the transition point. Therefore, we can use the quantities $c(T)$ and $\lambda_r(T)$ averaged over a long time to evaluate the transition point T^*; we again denote such quantities by the same notations $c(T)$ and $\lambda_r(T)$.

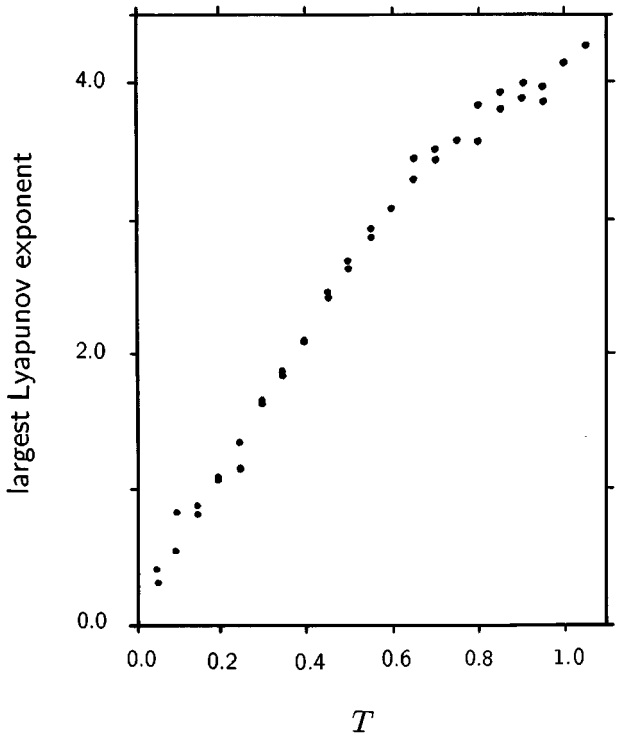

FIG. 7. The largest Lyapunov exponent as a function of T, calculated for the LJ system of $N=108$ and $d=3$ for the random configurations of the basins. The unit of the horizontal axis is the energy unit ϵ_0 [appearing in Eq. (2)], while that of the vertical axis is $1/\Delta_t$, where Δ_t is the time unit; $\Delta_t=0.01\sqrt{\{l^2\epsilon_0/m\}}$. The magnitude of the largest Lyapunov exponents is insensitive to the system size N; the result for $N=108$ is identical to that $N=256$ or 500.

Let us compare the expression in Eq. (34) with the results of computer simulations for the Lennard-Jones system of $N=108$. The interaction potential is given in Eq. (4). The calculated $\lambda_r(T)$ and $D_q(T)$ are shown in Figs. 7 and 8, as a function of T. The calculated $\lambda_r(T)$, the largest Lyapunov exponent, is about $\lambda_r(T)\sim 5.8T$ for $0<T<0.75$, while for $0.4\leqslant T$, the diffusion constant $D_q(T)$ is described by the Arrhenius law,

$$D_q(T)\simeq 0.12\sqrt{T}e^{-2.13/T}. \tag{36}$$

The calculated $c(T)$ has been already given in Eq. (9): $c(T)=\sqrt{T}e^{-2.16/T}/5.82$. By inserting the calculated $D_q(T)$ and $c(T)$ into Eq. (35), the size l_q^2 of the basin is estimated to be $0.698e^{0.03/T}$: the weak T dependence of the estimated size is regarded as negligible within the error of the computer simulations. From this, we have the reasonable basin size $l_q\simeq 0.8354$, which is close to the distance ($\simeq 0.77$) between the nearest neighboring particles for the fcc structure.

Let us evaluate the transition point T^* satisfying the equation $\sigma(T^*)=1$. The value of $r_{p,p'}(0)$ is necessary to evaluate $\sigma(T)$ in Eq. (34). However, it is not determined within the

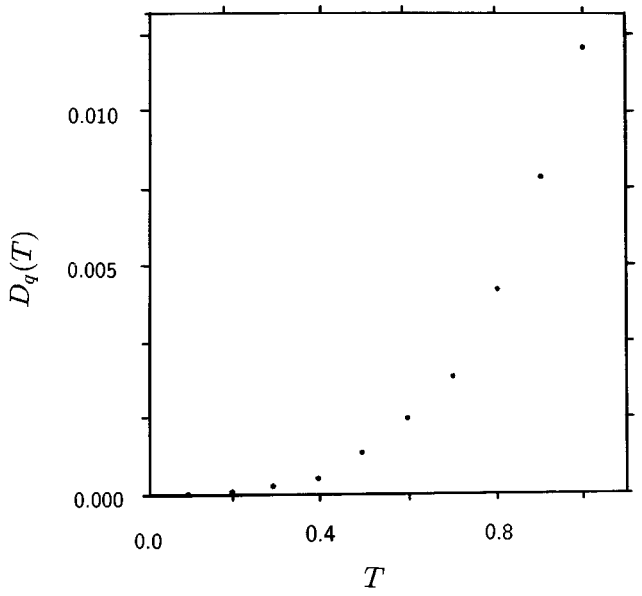

FIG. 8. The diffusion constant $D_q(T)$ as a function of T, calculated for the LJ system of $N=108$ and $d=3$ for the random configurations. The unit of the horizontal axis is the energy unit ϵ_0 [appearing in Eq. (2)], and that of the vertical axis is the length unit l [appearing in Eq. (2)]. The magnitude of the diffusion constant is insensitive to the system size N; the result for $N=108$ is identical to that of $N=500$ or 864.

framework of classical mechanics. Here, we make the semiclassical ansatz given by $r_{p,p'}(0)=h/L$, where L is the system size and h is the Planck constant. The choice of system size L reflects less on the value of T^*. For example, for system size $L=1$ cm, $\ln(r_{p,p'}(0))\simeq -18.885\,064\,937\,546\,1$ in our units. The τ_p and τ_q given in Eqs. (26) and (33) are shown in Fig. 9 as a function of T. The τ_p's are calculated

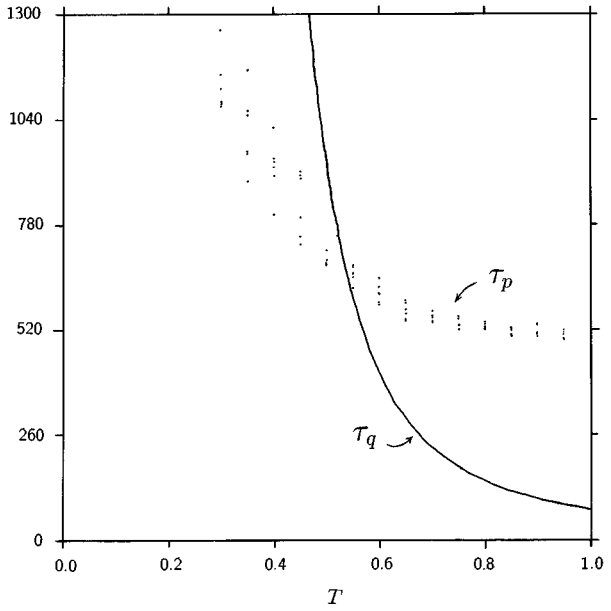

FIG. 9. τ_p and τ_q as a function of T for the LJ system of $N=108$ and $d=3$. The unit of the horizontal axis is the energy unit ϵ_0 [appearing in Eq. (2)], and that of the vertical axis is the time unit Δ_t $(=0.01\sqrt{\{l^2\epsilon_0/m\}})$.

for ten initial conditions. τ_q depends on T more rapidly than does τ_p. This rapid dependence determines the position at which the curve of τ_p crosses that of τ_q. From this figure, we have the transition point $T^*\simeq 0.48$.

In order to confirm the validity of our theoretical conclusion, we performed computer simulations for five initial conditions by changing T to examine whether the asymmetric motion appears or not. The simulation results determined for the five initial conditions are $T^*\simeq 0.55$, $T^*\simeq 0.55$, $T^*\simeq 0.50$, $T^*\simeq 0.50$, and $T^*\simeq 0.50$. These agree well with our theoretical result $T^*\simeq 0.48$.

B. Truncated Lennard-Jones system: Case of $N=32$

Let us test our assertion for another system, a Lennard-Jones type where the interaction potential is given by

$$v(q)=A(q^{-12}-1)e^{1/(q-q_0)} \quad (0<q<q_0),$$
$$=0 \quad (q_0\leqslant q), \tag{37}$$

where $A=8.805\,977$ and $q_0=1.652\,194$. The units of time, energy, length, and mass are assumed to be the same as those for Ar atoms. This system has been examined by Stillinger and Weber [10]. They have calculated the number of transitions between the basins during 10 000 time steps in their molecular dynamics. They assumed the time unit $\Delta_t=0.001\,25$, and the system size $N=32$. By changing the time unit Δ_t from 0.001 25 to 0.01 and by using the relation $s(t)=Nc(T)t$, we have $c(T)$ given by

$$c(T)\simeq \frac{\sqrt{T}}{126.325}\, e^{-2.163/T}. \tag{38}$$

For this system, we calculated τ_p as a function of T (τ_p and τ_q are plotted in Fig. 10 as a function of T). τ_q depends on T more rapidly than does τ_p. This rapid dependence determines the position at which the curve of τ_p crosses that of τ_q. From this figure, we theoretically obtain the transition point $T^*\simeq 1.6$–1.7. Here we used $r_{p,p'}(0)=h/L$, where h is the Planck constant and $L=1$ cm. On the other hand, using the results of the computer simulation performed by Stillinger and Weber, we have $T^*\simeq 1.6$ [10]. This agrees well with our theoretical result $T^*\simeq 1.6$–1.7.

For this system, we also calculated the diffusion constant $D_q(T)$ to give

$$D_q(T)\simeq \frac{\sqrt{T}}{256.4}\, e^{-2.16/T} \tag{39}$$

for the region $1.3<T\leqslant 3.0$. By inserting this and $c(T)$ in Eq. (38) into Eq. (35), we have a reasonable basin size, $l_q^2\simeq 0.49e^{0.03/T}$ or $l_q\simeq 0.7e^{0.015/T}$, which is close to 0.77, the distance between the nearest neighboring particles of the fcc structure. The weak T dependence of the estimated size is regarded as negligible within the error of the computer simulations.

In this section, we have confirmed our assertion that the T^* satisfying the $\sigma(T^*)=1$ in Eq. (34) is the transition point that determines whether or not asymmetric motion occurs. The transition points calculated by using the largest Lyapunov exponents and $c(T)$ are in excellent agreement

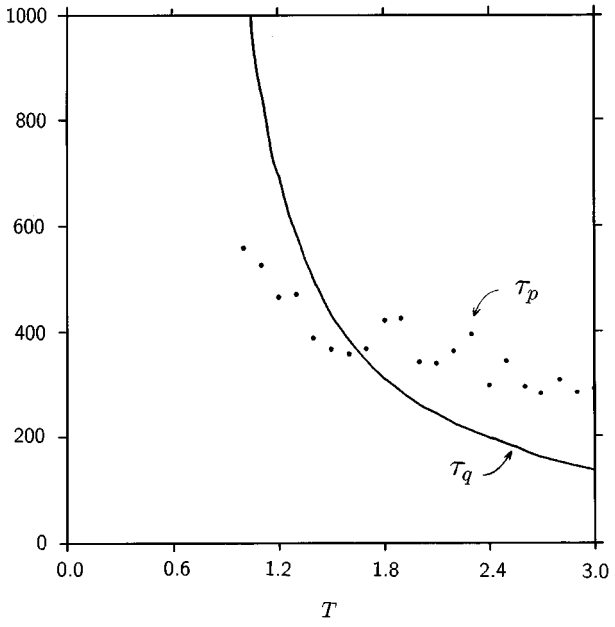

FIG. 10. τ_p and τ_q as a function of T for the truncated LJ system of $N=32$ and $d=3$, similar to Fig. 9. The units of the horizontal and vertical axes are the same as those in Fig. 9. τ_q was obtained by modifying the result by Stillinger and Weber. τ_p is calculated here for $N=108$; it is found that the magnitude of τ_p is insensitive to the number N of particles.

with the results obtained by performing computer simulations for two types of interaction potential. Furthermore, it was found that the expression for basin size obtained by applying the phenomenological arguments, which is given in Eq. (34), yields reasonable basin sizes.

VI. CONCLUSIONS AND DISCUSSION

A. Summary

We have studied the dynamical properties of Hamiltonian systems having a many-basin structure. The many-basin structure of the potential surface produces a variety of phase dynamics, i.e., the motion among basins and the motion within a basin. The motion within a basin has been studied with two types of the particle configurations, i.e., ordered and random. For the ordered configurations, the collapse of the KAM torus occurs at the finite kinetic energy T_0^c. For the sufficiently small kinetic energy $0<T\leqslant T_0^c$, the phase point is trapped on the KAM torus corresponding to the fcc ordered configuration. This finite stochastic transition has been also found for one- or two-dimensional systems with single-basin structures such as the Fermi-Pasta-Ulam model, the Lennard-Jones model, and so on. On the other hand, for random configurations, stochasticity occurs for even sufficiently small kinetic energy. Due to the fact that most basins have random configurations, the chaotic sea may prevail over most of the available Γ space. From this, it is suggested that the phase point may move around the various basins.

The motion of phase point among basins is classified into three types of motions, depending upon the magnitude of kinetic energy. These are further classified according to whether or not asymmetric motion occurs. The dynamic origin of the asymmetric motion is clarified by introducing the notion of intensity of motion in phase space, the degree of which is measured by $\sigma(T)=\tau_p(T)/\tau_q(T)$, where $\tau_p(T)$ is the time scale during which mixing is accomplished in the momentum space, while $\tau_q(T)$ is the time scale during which the phase point passes over the given basin. The asymmetric motion is attributed to the transient formation of the canonical probabilistic measure. The $\sigma(T)$ is expressed in terms of the dynamical quantities. Our assertion is confirmed by performing the numerical calculations that T^* satisfying $\sigma(T^*)=1$ is the transition point of whether or not the asymmetric motion occurs. For the occurrence of asymmetric motion, the relaxation dynamics in the momentum space are completed faster than the diffusion dynamics in the coordinate space, causing the dynamics to proceed so as to increase phase space volume Ω or entropy for the momentum space. This is the reason why the ordered phase emerges among many random configurations. The notion of intensity of motion is expected to help in discovering a generation principle of ordered phases of condensed matter out of many configurations.

B. Other properties of type 3

The following dynamical properties are observed in addition to intermittency and asymmetric motion.

(a) Strong dynamical instability during the intermittent transition. The absolute diffusion length, $a_q(t)$ of the phase point, grows exponentially with time t,

$$a_q(t)\simeq a_q(0)e^{\lambda_r^a t}, \tag{40}$$

where $a_q(t)$ is defined by

$$a_q(t)^2=\frac{1}{Nd}\sum_{j\alpha}|q_{j\alpha}(t)-q_{j\alpha}(0)|^2. \tag{41}$$

This is defined for the single trajectory, being sensitive to the trajectory (the initial condition). The intermittent transition occurs fast. The instability rate λ_r^a is a few or several times greater than the largest Lyapunov exponent for the motion of phase point staying within a basin. The $a_q(t)^2$ grows exponentially with time during the intermittent transition, which should be in contrast to that for the normal diffusion in which it increases linearly with time. The absolute diffusion length during the intermittent transition is shown in Fig. 11 as a function of time t. The intermittency occurs from $t=10\,000$ to 10 250. The exponential growth of $a_{p,q}(t)$ on t in Fig. 11(a) is ambiguous since the momentum part, $a_p(t)$, rapidly oscillates, as shown in Fig. 11(b). By excluding this rapidly oscillating part from $a_{p,q}(t)$, the exponential dependence becomes clear, as shown in Fig. 11(c).

(b) Many-transition-path formation. The phase points with two different initial conditions, $\{p_i(0),q_i(0)\}$ and $\{p_i'(0),q_i'(0)\}$, set in a given basin follow different transition paths. This property means that there are many transition paths starting from the given basin. The dynamics follows the different paths, indicating the formation of a many-transition path.

The following three properties (c), (d), and (e) are seen from Fig. 12.

(c) Easy-path formation. A few particles move along the line topology in the three-dimensional real space; only these

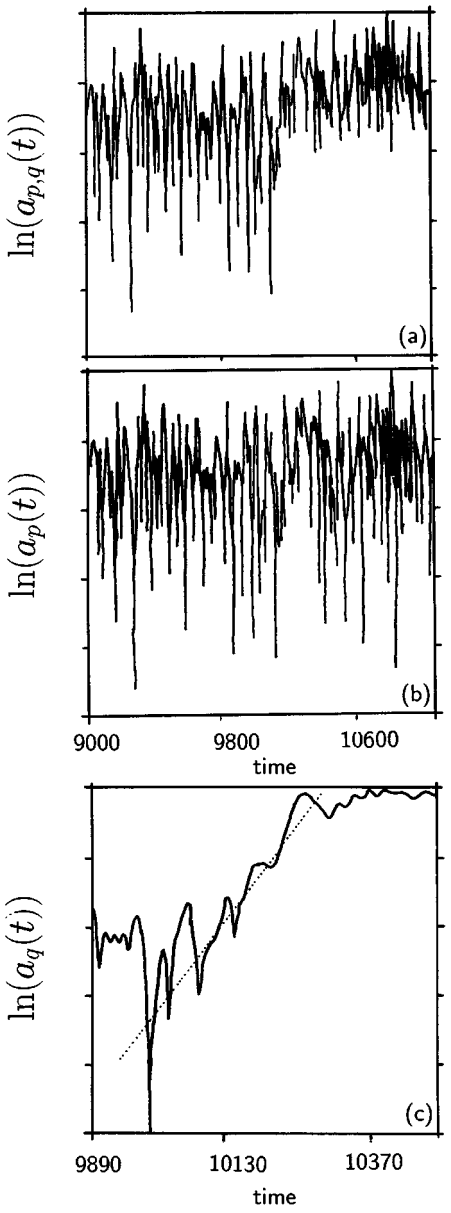

FIG. 11. (a) Logarithm of the absolute diffusion length during the intermittent transition for $N=108$. The unit of the horizontal axis is the time unit Δ_t $(=0.01\sqrt{\{l^2\epsilon_0/m\}})$, and the unit of the vertical axis is obtained by using the length unit l [appearing in Eq. (2)] but is arbitrary. The intermittent transition occurs from $t=10\,000$ to 10 250. The phase point stays in one local minimum for $t<10\,000$, and stays in another local minimum for $10\,250<t$. The absolute diffusion lengths are defined by $a_{p,q}(t)^2 = a_p(t)^2 + a_q(t)^2$, where $a_p(t)^2$ is the momentum part defined by $a_p(t)^2 = \Sigma_i |p_i(t) - p_i(0)|^2/3Nd$, and $a_q(t)^2$ the coordinate part, defined by $a_q(t)^2 = \Sigma_i |q_i(t) - q_i(0)|^2/3Nd$. From this figure, the exponential growth of $a_{p,q}(t)$ is ambiguous. (b) Logarithm of momentum diffusion length, $\ln(a_p(t))$, rapidly oscillates and is similar to (a). The time intervals observed in the top and center figures are the same but different from that in the bottom figure. (c) Logarithm of a coordinate diffusion length $\ln(a_q(t))$. The function of $\ln(a_q(t))$ is linear between $t=10\,000$ and 10 250, showing the exponential dependence of $a_q(t)$. The dotted line is a guide for the eye.

seem to move before the transition occurs. This implies that the potential barrier is finite, being irrelevant to the system size.

(d) Cascade collapse: the other remaining particles follow the motion of a few particles. This implies that the transition occurs between two basins whose spatial distance is remote.

A change of particle configuration is caused by the intermittent transition occurring at about $t=3800$ in the figure. The configuration of particles in the cube looked at from the y axis is indicated. The coordinates of particles are given by $\{x_i, y_i, z_i\}$. The configuration (at the local minimum) before the intermittent transition is indicated by particles shown by green circles, while that after the intermittent transition is indicated by particles shown by red circles. The red lines indicate a change of coordinate for particles during intermittent transition. The large (or small) change is indicated by the bold (or solid) red lines. The bold lines form the line topology, suggesting an easy-path formation. By studying the time-dependent diffusion length of each particle, it is found that the intermittent transition occurs as follows: particles 81 and 82 move first. Particles 9 and 26 move; particle 9 moves to fill a hole left after the movement of 81, and particle 26 is pushed up by particle 82. Subsequently, particles 61 and 75 move. Finally, the other remaining particles relax into the next stable configuration. Just a few particles move before transition, suggesting that the potential barrier is finite, irrelevant to the system size, and cascade collapse. The other remaining particles follow the motion of these particles, suggesting that there arises a transition between two stable configurations whose distance is remote. This, however, does not imply that a few particles trigger transition. The other particles can be considered to prepare their local motion. For these motions, it seems difficult or even meaningless to answer the question of what triggers the motion. The transition motion of type 3 is different from the Arnol'd diffusion and the induction phenomenon because type 3 is chaotic.

There are other types of particle dynamics during intermittent transition. For example, two particles move at the same time before the other particles follow. It is often observed that a few particles move before the others follow them.

(e) Complex connectivity of transition paths.

The motion of type 3 relates to the complex connectivity of the transition path between basins. The phase point assumes the value V_i intermittently during transition. The potential energy is shown in Fig. 13(a) along the shortest path (straight line) connecting two local minima of basins between which the intermittent transition occurs. The broken line indicates the potential energy along this line. The bold line indicates which basin the spatial point along the shortest path belongs to. It is noted that some V_i's are different from those of the initial and final basins. This means that some basins intersect between the initial and final basins. The schematic landscape of the potential surface is shown in Fig. 13(b). The intermittency bypasses the basins' intersecting. The complex connectivity of the transition path causes the intermittency. This is in contrast to the motions of types 1 and 2; no other basin intersects with the initial and final basins between which the motion of the phase point occurs actually. One of the indices used to measure the complexity of the transition paths is the number of other basins intersecting between the initial and final basins.

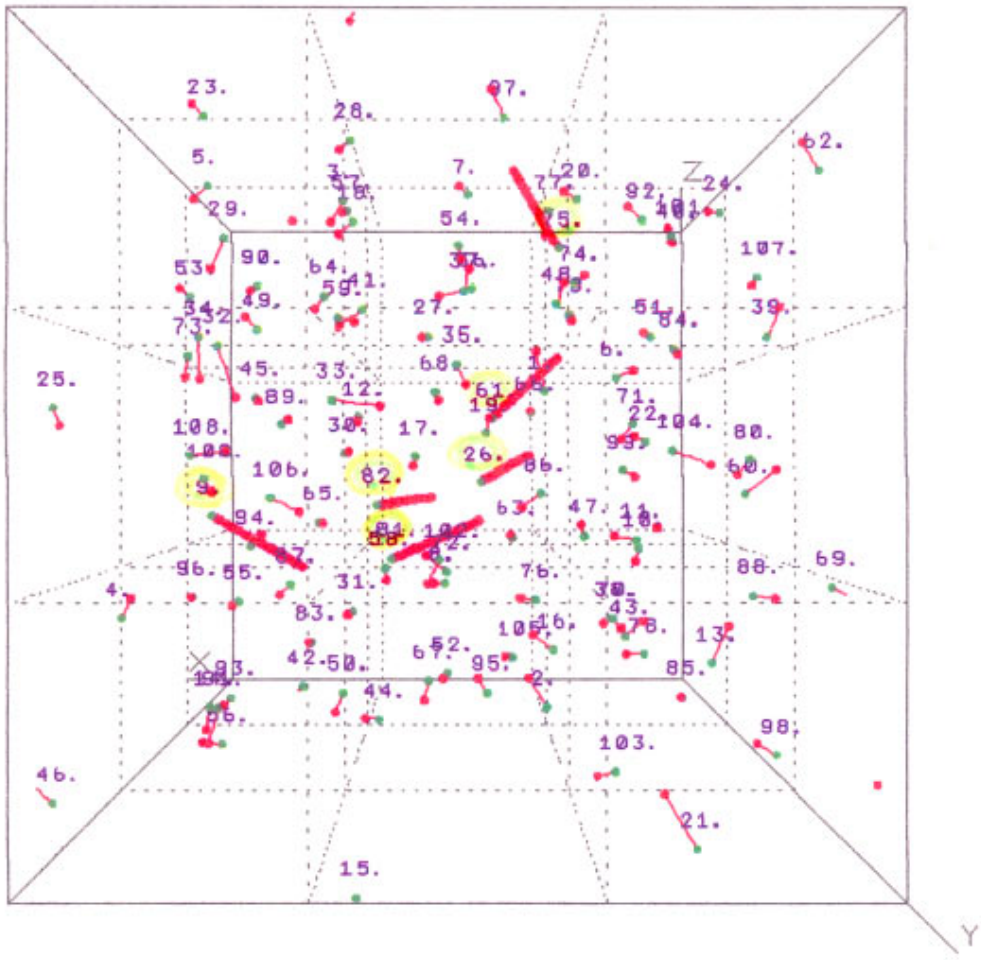

FIG. 12. A change in particle configuration caused by the intermittent transition occurring at about $t=3800$ in Fig. 4(c) for $N=108$. The configuration of particles in the cube viewed from the y axis is indicated. The coordinates of particles are given by $\{x_i, y_i, z_i\}$. The configuration (at the local minimum) before intermittent transition is indicated by particles shown by green circles, while that after the intermittent transition is indicated by particles shown by red circles. The red lines indicate change in the coordinates of particles during intermittent transition. The large (or small) change is indicated by the bold (or solid) red lines. The bold lines form the line topology, suggesting an easy-path formation. By studying the time-dependent diffusion length of each particle, it has been found that the intermittent transition occurs as follows: particles 81 and 82 move first. Particles 9 and 26 then move; particle 9 moves to fill a hole left after the movement of 81, and particle 26 is pushed up by particle 82. Subsequently, particles 61 and 75 move. Finally, the other remaining particles relax into the next stable configuration. This analysis implies some properties: Localness: just a few particles move before transition, suggesting that the potential barrier is finite and unrelated to the system size; Cascade collapse: the other remaining particles follow the motion of a few particles, suggesting that there is a transition between two transiently stable configurations whose distance is remote.

The intermittent transitions are observed [35,36] for many dissipative and conservative systems with many degrees of freedom, similar to type 3.

C. Directions for future work

The major problems remaining in this work are listed here:

(1) For investigating the asymmetric motion, we used the concept of ensemble of the trajectories for the mixing dynamics in the momentum space. This use challenges a picture of the phase point moving in the phase space.

(2) There is an asymmetry that causes the time scales τ_p and τ_q to be incorporated into the expression of $\sigma(T)$. τ_p is concerned with the mixing dynamics in the momentum space, while τ_q is concerned with the diffusion dynamics in the coordinate space. The mixing is concerned with the ensemble of trajectories, whereas the diffusion is concerned with a single trajectory. Why does this asymmetry appear?

(3) The asymmetric motion has been discussed on the basis of the many-basin structure. The celestial systems or Coulombic systems may have no many-basin structure. Are our arguments for the asymmetric motion valid for these systems? How can we expand our arguments to these systems?

ACKNOWLEDGMENTS

We would like to thank S. Tasaki, K. Ikeda, K. Kaneko, and P. Davis for their stimulating discussions.

APPENDIX

The equations of motion for $\{p^0_{j\alpha}(t_i), q^0_{j\alpha}(t_i)\}$ and $\{p_{j\alpha}(t_i), q_{j\alpha}(t_i)\}$ $(j=1,\ldots,N;\ \alpha=1,\ldots,d)$ at time $t_i=t_0+i\Delta_t$

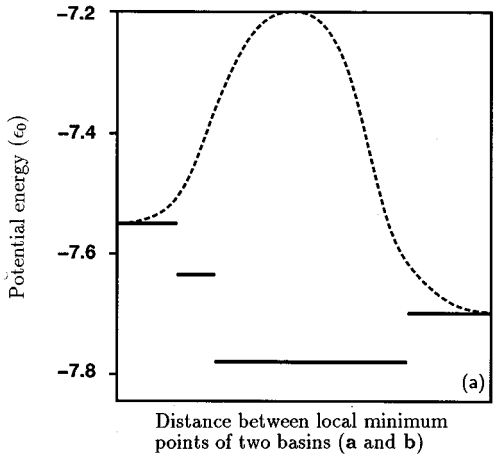

Illustration of landscape of the potential energy between two basins (a and b) corresponding to the above figure, similar to Fig.1

FIG. 13. (a) Plot of the potential energy on the shortest path connecting the local minima of two basins between which phase transition actually occurs for the LJ system of $N=108$, indicated by the broken line. The bold lines indicate which basin the spatial point along the shortest path belongs to. There are some V_i's which are different from those of the initial and final basins. This means that there exist some basins intersecting between the initial and final basins. The length unit of the horizontal axis is taken as arbitrary, and the unit of the vertical axis is the energy unit ϵ_0 [appearing in Eq. (2)]. (b) Complex connectivity of the transition path among basins for the motion of type 3, corresponding to the intermittent transition in (a). Similar to Fig. 1, the schematic landscape of the many-dimensional potential surface $V[q_{j\alpha}]$ is shown. The intermittency bypasses the intersecting basins. The complex connectivity of the transition path causes the intermittency. This is in contrast to the case of motions of types 1 and 2; no other basin with the initial and final basins (indicated by the shaded region) between which the motion of phase point actually occurs.

where t_0 is the initial time and Δ_t is the time step, is given by the following Euler equation:

$$q^0_{j\alpha}(t_{i+1})=q^0_{j\alpha}(t_i)+\Delta_t p^0_{j\alpha}(t_i),$$

$$p^0_{j\alpha}(t_{i+1})=p^0_{j\alpha}(t_i)+\Delta_t \sum_{k(\neq j)\beta} q^0_{k\beta}(t_{i+1}) f^0_{j\alpha k\beta}, \quad \text{(A1)}$$

$$q_{j\alpha}(t_{i+1})=q_{j\alpha}(t_i)+\Delta_t p_{j\alpha}(t_i),$$

$$p_{j\alpha}(t_{i+1})=p_{j\alpha}(t_i)+\Delta_t \sum_{k(\neq j)\beta} q_{k\beta}(t_{i+1}) f_{j\alpha k\beta}, \quad \text{(A2)}$$

where

$$f^0_{j\alpha k\beta}=-\frac{\partial^2 v[q^0_{l\gamma}(t_{i+1})]}{\partial q^0_{j\alpha}(t_{i+1})\partial q^0_{k\beta}(t_{i+1})}$$

$$f_{j\alpha k\beta}=-\frac{\partial^2 v[q_{l\gamma}(t_{i+1})]}{\partial q_{j\alpha}(t_{i+1})\partial q_{k\beta}(t_{i+1})}. \quad \text{(A3)}$$

The equation for the time evolution of the quantities $\{\delta p_{j\alpha}(t_i),\delta q_{j\alpha}(t_i)\}$ along the trajectory $\{p^0_{j\alpha}(t_i),q^0_{j\alpha}(t_i)\}$, where $\delta p_{j\alpha}(t_i)=p_{j\alpha}(t_i)-p^0_{j\alpha}(t_i)$ and $\delta q_{j\alpha}(t_i)=q_{j\alpha}(t_i)-q^0_{j\alpha}(t_i)$, is obtained from Eqs. (A 1) and (A 2) by assuming that $\delta p_{j\alpha}(t_i)$ and $\delta q_{j\alpha}(t_i)$ are sufficiently small:

$$\delta q_{j\alpha}(t_{i+1})=\delta q_{j\alpha}(t_i)+\Delta_t \delta p_{j\alpha}(t_i), \quad \text{(A4)}$$

$$\delta p_{j\alpha}(t_{i+1})=\delta p_{j\alpha}(t_i)+\Delta_t \sum_{k(\neq j)\beta} \delta q_{k\beta}(t_{i+1}) f^0_{j\alpha k\beta},$$

$$=\delta p_{j\alpha}(t_i)+\Delta_t^2 \sum_{k(\neq j)\beta} p_{k\beta}(t_i) f^0_{j\alpha k\beta}$$

$$+\Delta_t \sum_{k(\neq j)\beta} q_{k\beta}(t_i) f^0_{j\alpha k\beta}. \quad \text{(A5)}$$

Here, we used Eq. (A4) to get the final equation in Eq. (A5). Equations (A4) and (A5) are rewritten symbolically as

$$\begin{pmatrix}\delta p_{j\alpha}(t_{i+1})\\ \delta q_{j\alpha}(t_{i+1})\end{pmatrix}=G[p^0_{j\alpha}(t_{i+1}),q^0_{j\alpha}(t_{i+1})]\begin{pmatrix}\delta p_{j\alpha}(t_i)\\ \delta q_{j\alpha}(t_i)\end{pmatrix}. \quad \text{(A6)}$$

As seen from Eqs. (A4) and (A5), the Jacobian of the transformation matrix from $\{\delta p_{j\alpha}(t_i),\delta q_{j\alpha}(t_i)\}$ to $\{\delta p_{j\alpha}(t_{i+1}),\delta q_{j\alpha}(t_{i+1})\}$ is equal to unity, ensuring the area preserving property of the shift map $G[p^0_{j\alpha}(t_{i+1}),q^0_{j\alpha}(t_{i+1})]$. The growth rate, the largest Lyapunov exponent of the time evolution $\{\delta p_{j\alpha}(t_i),\delta q_{j\alpha}(t_i)\}$ along the trajectory $\{p^0_{j\alpha}(t_i),q^0_{j\alpha}(t_i)\}$, is obtained as the limiting value $(i\to\infty)$ of the quantity $\lambda(i)$, which is defined by

$$\lambda(i)=\frac{1}{2i\Delta_t}\sum_{n=1}^{i} \ln \mathrm{Tr}\{{}^tG[p^0_{j\alpha}(t_{n+1}),q^0_{j\alpha}(t_{n+1})]$$

$$\times G[p^0_{j\alpha}(t_{n+1}),q^0_{j\alpha}(t_{n+1})]\}. \quad \text{(A7)}$$

Here, we used the notation i to express the time. The symbol $\mathrm{Tr}[x]$ means the trace of the matrix x, and the suffix t on the left shoulder of the matrix stands for its transpose. As discussed in the text, there is a possibility that the phase point may escape from the basin during a long run and for a larger kinetic energy. The growth rates λ of the time evolution of the trajectories are calculated for the time interval within

which the phase point stays in the single basin, i.e., for the typical $i \leqslant 200$, and are averaged over the many different trajectories starting with phase points $\{p^0_{j\alpha}(t_i), q^0_{j\alpha}(t_i)\}$ confined in the single basin.

The Lyapunov spectra can be obtained as the growth rates of the orthonormal vectors spanned in the Γ space, whose number is $2Nd$. The equation of motion they obey is given by Eq. (A 6). They become nonorthonormalized as the dynamics proceed. Then a new set of orthonormal vectors are obtained by using Schmidt's orthogonalization technique. By using this procedure repeatedly, we have the Lyapunov exponents averaged along the trajectory $\{p^0_{j\alpha}(t_i), q^0_{j\alpha}(t_i)\}$.

[1] J. C. Phillips, Phys. Rev. B **46**, 8542 (1992).
[2] J. C. Langer, Phys. Today **10**, 24 (1992).
[3] P. W. Anderson, *Concepts in Solids* (W. Benjamin, Reading, MA, 1963).
[4] S. Aubry, J. Phys. (Paris) **44**, 147 (1983).
[5] F. H. Stillinger and T. A. Weber, Phys. Rev. A **25**, 978 (1982).
[6] Shinjo Kazumasa, Phys. Rev. B **40**, 9167 (1989); J. Chem. Phys. **90**, 6627 (1989).
[7] N. S. Krylov, in *Works on the Foundations of Statistical Physics* (Princeton University Press, Princeton, NJ, 1979), pp. 193–206.
[8] F. G. Amar and R. S. Berry, J. Chem. Phys. **85**, 5943 (1986).
[9] J. Jellinek, Adv. Chem. Phys. **70**, 75 (1988).
[10] F. H. Stillinger and T. A. Weber, Phys. Rev. B **28**, 2408 (1983); Science **225**, 983 (1984).
[11] L. Verlet, Phys. Rev. **159**, 98 (1967).
[12] P. Bocchieri, Phys. Rev. A **2**, 2013 (1970).
[13] M. C. Carotta, C. Ferrario, G. LoVecchio, and L. Galgani, Phys. Rev. A **17**, 786 (1978).
[14] M. Casartelli, E. Diana, L. Galgani, and A. Scotti, Phys. Rev. A **13**, 1921 (1976).
[15] M. Pelti, Phys. Rev. E **47**, 828 (1993).
[16] G. Benettin, in *Proceedings of the International School of Physics, ''Enrico Fermi,''* Course XCVII, edited by G. Ciccotti and W. Hoover (North-Holland, Amsterdam, 1988), p. 15.
[17] G. Benettin, Prog. Theor. Phys. Suppl. **116**, 207 (1994).
[18] B. P. Wood, A. J. Lichtenberg, and M. A. Lieberman, Physica D **71**, 132 (1994).
[19] E. Fermi, J. Pasta, and S. Ulam, in *S. Ulam: Sets, Numbers, and Universes*, edited by W. A. Berger *et al.* (MIT Press, Cambridge, MA, 1974), p. 490.
[20] F. M. Izrailev and B. V. Chirikov, Dokl. Akad. Nauk SSSR **166**, 57 (1966) [Sov. Phys. Dokl. **11**, 30 (1966)].
[21] P. Bocchieri, A. Scotti, B. Bearzi, and A. Loinger, Phys. Rev. **2**, 2013 (1970).
[22] L. Boltzmann, Wiedemann Ann. **57**, 773 (1896).
[23] J. H. Jeans, Philos. Mag. **6**, 279 (1903); **10**, 91 (1905).
[24] G. Benettin, L. Galgani, and A. Giorgilli, Phys. Lett. A **26**, 23 (1987).
[25] G. Benettin, G. LoVecchio, and A. Tenenbaum, Phys. Rev. A **22**, 1709 (1980).
[26] G. Benettin and A. Tenenbaum, Phys. Rev. A **28**, 3020 (1983).
[27] Y. Hagihara, in *Celestial Mechanics* (Japan Society for the Promotion of Science, Tokyo, 1976), Vol. 2, p. 1245.
[28] M. von Smolukhovsky, Ann. Phys. (Leipzig) **21**, 756 (1906).
[29] L. Boltzmann, Nature (London) **51**, 413 (1895).
[30] For $N=108$, all behaviors of V_i are classified into three types of motion, provided that the initial configuration is random. Figures 4(a)–4(c) show typical behaviors of V_i, corresponding, respectively, to the cases of higher, intermediate, and lower T. This classification was found by calculating a series of V_i for the 30 trajectories. For the smaller system of $N=32$, the classification becomes intermediate. For the larger systems of $N=256$ and 864, we were unable to calculate V_i with our limited computer power. Instead, we calculated T as a function of time, which characterizes the kinetic energy defined in Eq. (4). The quantity T continues to increase when the asymmetric motion occurs. The judgment of whether or not the asymmetric motion occurs is made by examining the time dependence of T. From this, we can conclude the existence of type 1 motion showing no increase in T. Next, we can confirm that the asymmetric motions are classified into two types (corresponding to types 2 and 3) as follows. For higher T, the dynamics show no asymmetric motion. By decreasing the initial kinetic energy T, the dynamics show asymmetric motion. Then T *gradually* increases as time elapses, suggesting that the phase point wanders from basin to basin. This is similar to the type 2 motion observed for $N=108$. By further decreasing the initial T, T intermittently increases as time elapses, corresponding to the type 3 observed for $N=108$. The frequency with which the basin depths are computed affects the details of the pattern shown in Figs. 4(a)–4(c). The wandering property, asymmetric motion, or intermittency observed for each type of motion, concluded from the patterns of V_i, do not depend on the details of the patterns. For example, the asymmetric motion for type 2 ceases after time goes beyond $\tau_2(N,T)$. The asymmetric motion and wandering property hold if many V_i's are calculated for the time t $[\leqslant \tau_2(N,T)]$.
[31] J. Lebowitz, Physica A **194**, 1 (1993); Phys. Today **9**, 32 (1993).
[32] V. I. Olesedec, Trans. Moscow Mathy. Soc. **19**, 197 (1978).
[33] E. Teramoto, in *Markovian Process and Dynamical Process* (Maki Shoten, Tokyo, 1961) p. 45,
[34] P. Klossowski, *Nietzsche et le Cercle Vicieux* (Mercure de France, Paris, 1969).
[35] K. Ikeda and K. Matsumoto, Physica D **29**, 223 (1987).
[36] I. Ohmine and H. Tanaka, Chem. Rev. **93**, 2545 (1993).